ELSEVIER

Journal of Power Sources 70 (1998) 78–84

JOURNAL OF POWER SOURCES

EIS study of electrochemical battery discharge on constant load

J.-P. Diard, B. Le Gorrec [*,1], C. Montella [2]

Ecole Nationale Supérieure d'Electrochimie et d'Electrométallurgie de Grenoble, Laboratoire d'Electrochimie et de Physicochimie des Matériaux et Interfaces, UMR 5631 CNRS–INPG, associée à l'UJF, Domaine Universitaire, BP 75, 38402 Saint-Martin-d'Hères, France

Received 27 January 1997; revised 17 May 1997; accepted 26 May 1997

Abstract

The impedance of electrochemical battery has been measured using a classical impedance-measurement apparatus to control the battery discharging into a constant load under current perturbation. This new method can be used even when the discharge current is greater than the maximum current that could be supplied by the regulation of the impedance-measurement apparatus used. Impedance measurements were first carried out on sealed Ni–Cd cells with a capacity of 0.65 Ah using the classical modulated current method and the new proposed method. The results show that the impedance diagrams, obtained during battery discharge through a constant load R, are identical to those obtained during discharges at a constant current with value U_{mean}/R where U_{mean} is the mean voltage of the battery during its natural discharge. These comparative measurements validate the proposed impedance-measurement method which can be used to test all types of batteries or fuel cells. Impedance measurements are presented for sealed lead/acid cells with a capacity of 25 Ah and battery discharge currents greater than the maximum current that the regulation system could supply. These measurements show that the proposed method may be used with classical impedance-measurement set to test high-capacity and low-impedance batteries during discharge into a constant load. © 1998 Elsevier Science S.A.

Keywords: Battery impedance spectroscopy; Nickel–cadmium cells; Lead/acid cells; Constant load discharge; Constant current discharge

1. Introduction

Impedance measurements provide useful information on electrochemical systems [1] and are proposed as a means of determining the state-of-charge of batteries. Classical impedance-measurement set implementing electrochemical regulation and a frequency response analyser can be used to measure the open-circuit impedance or the impedance during forced discharge of electrochemical batteries at a constant current. Under open-circuit conditions, the battery does not supply power during the experiment. It is thus possible to study, under potentiodynamic or intensiodynamic conditions [2–7], high- or low-capacity batteries or battery cells at different stages after charging or discharging. On the other hand, impedance measurements for charging or discharging batteries use a modulated current with an amplitude less than the maximum value (in general 2 A) of the regulation current. This explains why this method is used to measure the impedance of low-capacity batteries during operation [8]. Impedance measurement on cells in an operating telecommunication battery strings have alternatively been performed with a Fourier-transform signal analyser, using the intrinsic load and power supply induced noise of the operating battery string as a signal source [9].

We have developed a new experimental method to measure the impedance of batteries during discharge. This method uses classical impedance-measurement set to control, under sinusoidal current perturbation, a battery discharging into a constant load. In this case, the mean current flowing through the battery varies with time, however, the amplitude of the current modulation used for the impedance measurements, which is imposed by the electrochemical regulation, remains constant.

Examples of impedance measurements carried out on sealed Ni–Cd cells and sealed lead/acid cells, using the

* Corresponding author.

[1] Institut Universitaire de Technologie, Université Joseph Fourier de Grenoble, France.

[2] Institut des Sciences et Techniques, Université Joseph Fourier de Grenoble, France.

PII S0378-7753(97)02668-2

classical modulated-current method and the new proposed method, are presented. The results are compared for low-capacity batteries for which both methods may be used. Impedance measurements carried out using the new method, for cases in which the battery discharge current is greater than the maximum current that can be supplied by the regulation system, are presented for high-capacity batteries.

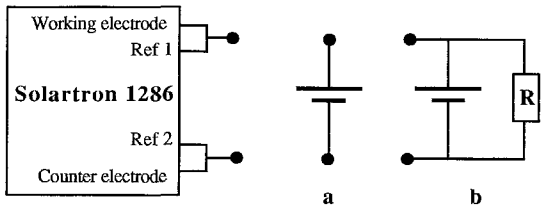

Fig. 1. Connections used for the EIS study during discharge of batteries at (a) constant current or (b) through a constant load.

2. Experimental method

The impedance measurements were carried out on batteries with different capacities, namely a Mazda sealed Ni–Cd type NCR6 0.65 Ah battery and a Hawker sealed lead/acid Cyclon type BC 25 Ah 2 V cell. The batteries underwent at least five charge/discharge cycles before testing.

The Ni–Cd batteries were charged under intensiostatic conditions according to the manufacturer's recommendations. We used a standard charge procedure corresponding to a 140% of the nominal capacity C, with a current corresponding to a 1 h capacity variation of $C/10$. Charging lasted approximately 14 h and the battery voltage was limited to 1.55 V. The sealed lead/acid batteries were charged at an imposed current level until a voltage of 2.3 V was reached, then this voltage was maintained constant until the battery was completely charged.

The batteries were discharged down to 0.9 V cut-off voltage for the Ni–Cd batteries and 1.8 V for the sealed lead/acid batteries.

The impedance measurements were carried out using an electrochemical-regulation system (Solartron 1286 electrochemical interface) and a Solartron 1250 frequency response analyser. The measurement set was controlled by a PC equipped with an HP 83200 IEEE board. The SAMDIE software developed in our laboratory [10] was used for data acquisition and plotting of impedance diagram. The results were processed using Mathematica™ [11] software.

Battery impedance was measured in the 6500 Hz–50 mHz or the 650 Hz–50 mHz frequency range, depending on the implemented current-measurement range, in automatic sweep mode from high to low frequency with 8 points per logarithmic decade. A low-pass filter with a 10 Hz cut-off frequency automatically steps in for frequencies under 1 Hz.

The Solartron 1286 regulation system was used in intensiodynamic mode in a two-electrode assembly. The reference 1 and working outputs on the regulation system were interconnected to constitute the positive output for the entire regulation system. The reference 2 and counter-electrodes outputs, interconnected, constituted the negative terminal for the regulation system. The connections between the battery and the regulation system are presented in Fig. 1(a) for battery impedance measurements during constant current discharge and in Fig. 1(b) for the study during constant load discharge.

3. Comparative study of low-capacity battery impedance during discharge at constant current or through a constant load

This study was carried out on low-capacity batteries in view of validating the new measurement method by comparing it to the classical method.

A battery may be characterized by its voltage change with time at an imposed discharge current. The value of this current may be expressed as 1 h capacity variation, for example $C/10$. The voltage variation can alternatively be expressed as a function of the discharge level given as a percentage of the nominal capacity. We used the latter representation because it may be used easily to compare two different discharge rates. We thus compared the discharge at constant current and the discharge through a constant load for a given battery.

Discharge of a battery through a constant load R is carried out with a current

$$I(t) = U(t)/R \quad (1)$$

which varies with the battery voltage $U(t)$. The mean discharge current I_{mean} is defined as

$$I_{mean} = [1/(Rt)]\int_0^t U(\tau)\mathrm{d}\tau \quad (2)$$

The change of the capacity Q(t) with time is then calculated by

$$Q(t) = (1/R)\int_0^t U(\tau)\mathrm{d}\tau \quad (3)$$

Alternatively, for a discharge at constant current I, we have

$$Q(t) = It \quad (4)$$

Fig. 2 shows the cell voltage evolution for a Mazda Ni–Cd type NCR6 0.65 Ah battery, discharged through a 30 Ω constant load as a function of the percentage of the nominal capacity calculated as

$$\%\ \text{capacity} = 100Q(t)/C \quad (5)$$

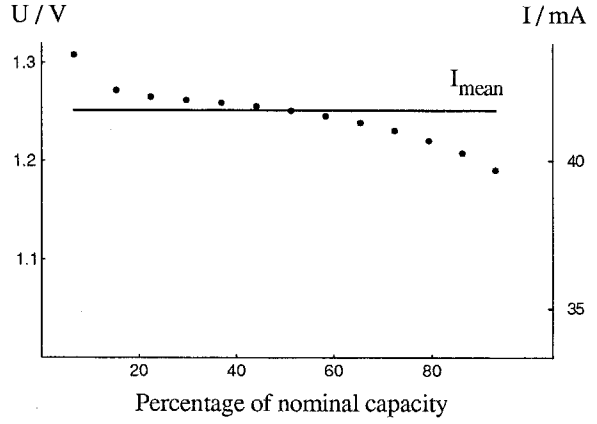

Fig. 2. Discharge of a Mazda Ni–Cd type NCR6 0.65 Ah battery through a 30 Ω constant load. Evolution of the battery voltage and the current during discharge as a function of the percentage of nominal capacity. The mean current discharge is given in full line.

Fig. 2 shows also the evolution of the discharge current and its mean value during discharge.

In Fig. 3, the voltage variation is compared with that of the same battery discharged at constant current. The discharge curves are approximately superimposable when the current used for discharge at constant current takes approximately the same value as the mean current observed for the natural discharge on the constant load.

The battery impedance was studied under sinusoidal current perturbation during discharges carried out with a current approaching $C/10$ over periods of at least 10 h. Using the condition of Fig. 1(a), the current imposed by the regulation system was the sum of a constant current I and a sinusoidal perturbation with a low amplitude ΔI. In contrast, the regulation system imposes only the sinusoidal current with amplitude ΔI when the battery impedance is measured during a discharge through a constant load (Fig. 1(b)).

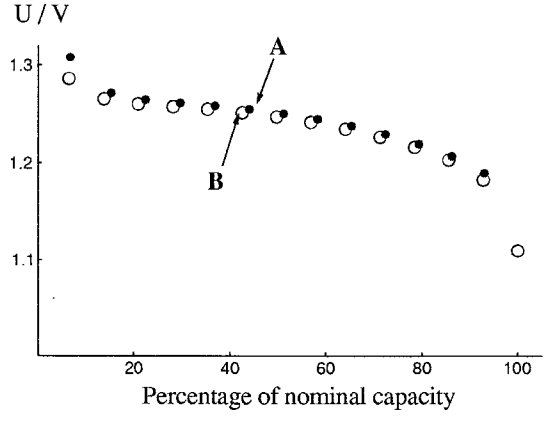

Fig. 3. Voltage evolution vs. percentage of nominal capacity for a Mazda Ni–Cd type NCR6 0.65 Ah. Battery discharged through (●) a 30 Ω constant load or (○) at a constant current $I = 42$ mA. Points A and B correspond to the impedance diagrams in Fig. 7 and Fig. 12.

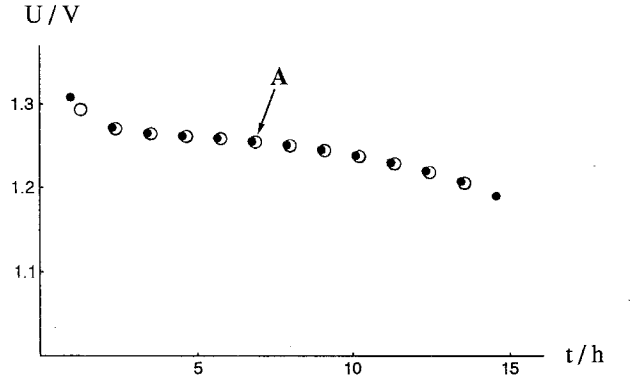

Fig. 4. Voltage evolution vs. discharge time for a Mazda Ni–Cd type NCR6 0.65 Ah battery (●) before and (○) after plotting of the impedance diagrams. Discharge through a 30 Ω constant load; $\Delta I = 2$ mA, $\nu \in$ 6500 Hz, 50 mHz. Point A corresponds to the impedance diagrams in Fig. 12.

Impedance measurements were carried out every hour and each diagram was obtained following a discharge of approximately 8% of nominal capacity. Integration of the signals corresponding to the current and the voltage was carried out by the frequency response analyser in automatic and long integration mode, with a maximum of 60 cycles on the measurement channel for the the battery voltage. Under these conditions, the acquisition time of an impedance diagram was approximately 7 min. Measurement of the battery voltage before and after plotting of the impedance diagram was used to check whether the battery operation was quasi-stationary. We noted that the voltage variation was less than 4 mV under the above experimental conditions, for a percentage of discharged nominal capacity between 10% and 90% (see Figs. 4 and 9).

The impedance diagrams show, at the highest frequencies, an inductive behaviour characteristic of the measure-

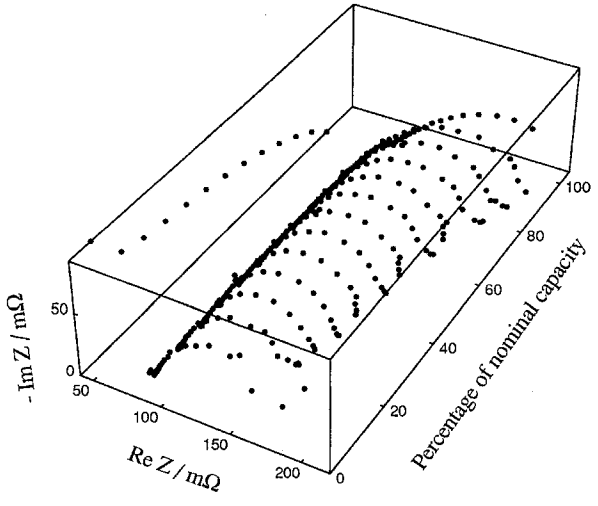

Fig. 5. Three-dimensional Nyquist representation of the impedance diagram evolution vs. percentage of nominal capacity for a Mazda Ni–Cd type NCR6 0.65 Ah battery after correction of the high frequency inductive part. Discharge through a 30 Ω constant load; $\Delta I = 2$ mA, $\nu \in$ 6500 Hz, 50 mHz. The battery voltage evolution during discharge is given in the profile plane.

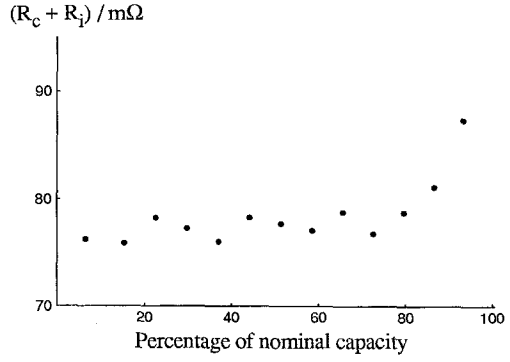

Fig. 6. $R_c + R_i$ evolution vs. percentage of nominal capacity for a Mazda Ni–Cd type NCR6 0.65 Ah battery discharged through a 30 Ω constant load.

ment set. The high-frequency part of the diagrams presented below was corrected using the procedure indicated in the Appendix.

Fig. 5 shows the Nyquist impedance diagrams for a Mazda Ni–Cd type NCR6 0.65 Ah battery discharging through a 30 Ω constant load as a function of the battery discharge level expressed as a percentage of its nominal capacity. The impedance diagrams, corrected in their high-frequency inductive part, are made up of two coalescent capacitive arcs in the 6500 Hz–50 mHz frequency range. The modulus of the battery impedance increases as the battery discharges.

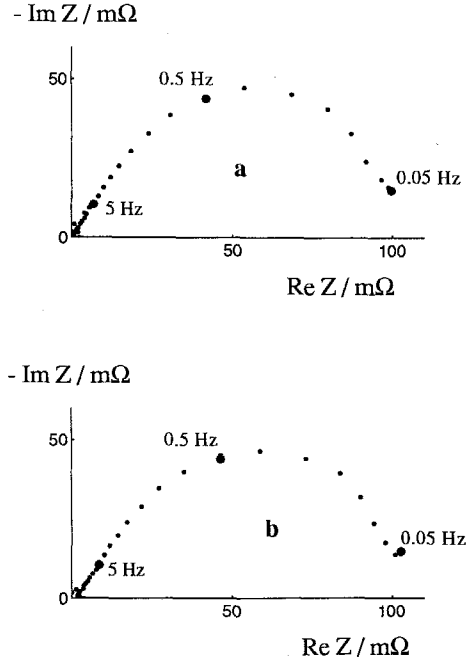

Fig. 7. Nyquist impedance diagrams for a Mazda Ni–Cd type NCR6 0.65 Ah battery after correction of the high frequency inductive and resistive parts: (a) at point A in Fig. 3 (discharge through a 30 Ω constant load), and (b) at point B in Fig. 3 (discharge at a constant current of 42 mA) with $\Delta I = 2$ mA, $\nu \in$ [6500 Hz, 50 mHz]. The frequency is indicated on the diagrams.

The impedance of the Ni–Cd battery may be roughly represented by combining a resistance R_c corresponding to the leads and the connections between the battery and the regulation system, an internal battery resistance R_i and the impedances of the electrodes which depend on the charge/discharge level of the battery. The value of $R_c + R_i$ is fairly constant during discharge and increases at the end of discharge (Fig. 6). This characteristic behaviour of the battery can be reproduced. However, the precise value of the resistance R_i for the battery cannot be determined accurately in this manner due to the non-reproducibility of the value for resistance R_c corresponding to the connections. We noted a dispersion of approximately 10% for the values of $R_c + R_i$ around a mean value for an identical discharge when the battery is disconnected, then reconnected between several identical experiments.

The corrected impedance diagrams for $R_c + R_i$, obtained using the two methods (discharge at constant current or through a constant load), are practically identical as shown in Fig. 7 in which two diagrams are shown corresponding to two similar discharge levels of the battery (points A and B in Fig. 3).

For a discharge carried out through a constant load R, the measured impedance $Z(\nu)$ is

$$Z(\nu) = Z_G(\nu)R/(Z_G(\nu) + R) \quad (6)$$

where $Z_G(\nu)$ is the battery impedance. The measured impedance is that of the battery provided

$$Z_G(\nu) \ll R \quad \forall \nu \in (\nu_{min}, \nu_{max}) \quad (7)$$

and therefore

$$Z(\nu) \approx Z_G(\nu) \quad \forall \nu \in (\nu_{min}, \nu_{max}) \quad (8)$$

which is satisfied for the discharge resistances used in this work.

The preceding comparative study shows that the battery impedance diagrams, obtained during discharges through a constant load R, are identical to those obtained during discharges at a constant current with a value equal to U_{mean}/R where U_{mean} is the mean battery voltage during

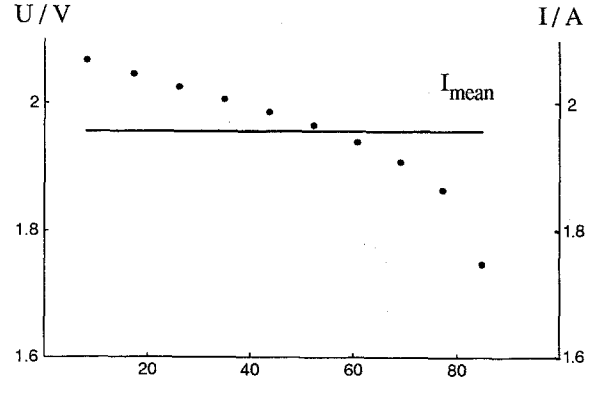

Fig. 8. Voltage and current evolutions vs. percentage of nominal capacity for a Hawker sealed lead/acid Cyclon type BC 25 Ah 2 V cell discharged through a 1 Ω constant load. The mean current discharge is given in full line.

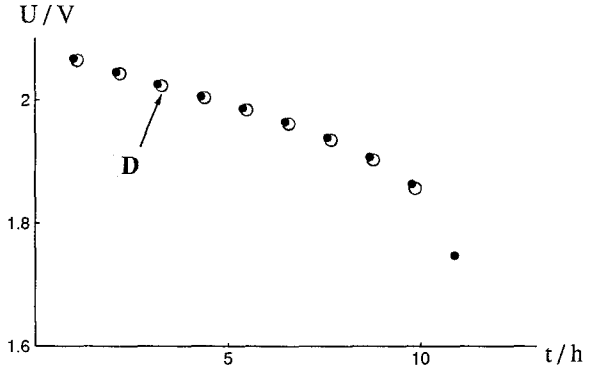

Fig. 9. Voltage of a Hawker sealed lead/acid Cyclon type BC 25 Ah 2 V cell (●) before and (○) after plotting of the impedance diagrams. Discharge through a 1 Ω constant load; $\Delta I = 60$ mA, $\nu \in$ [650 Hz, 50 mHz]. Point D corresponds to the impedance diagrams in Fig. 14.

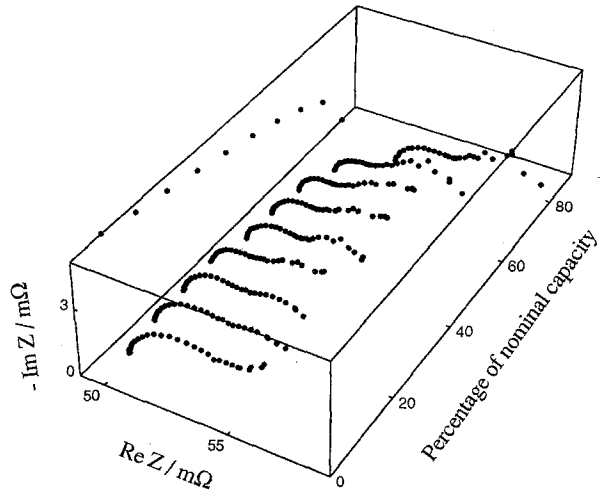

Fig. 10. Three-dimensional Nyquist representation of the impedance diagram evolution vs. percentage of nominal capacity for a Hawker sealed lead/acid Cyclon type BC 25 Ah 2 V cell after correction of the high frequency inductive part. Discharge through a 1 Ω constant load; $\Delta I = 60$ mA, $\nu \in$ [650 Hz, 50 mHz]. The battery voltage evolution during discharge is given in the profile plane.

its natural discharge. This study validates the new impedance-measurement method presented in this paper for a battery during discharge through a constant load.

4. Impedance of a high-capacity battery during discharge through a constant load

We measured the impedance of a Hawker sealed lead/acid Cyclon type BC 25 Ah 2 V cell during its discharge through a 1 Ω constant load for which the initial discharge current of 2.3 A was greater than the maximum value (2 A) that could be supplied by the regulation system. The constant-current measurement method could therefore not be implemented for such a high current. Fig. 8 shows the evolution of the battery voltage and the discharge current as a percentage of the nominal capacity. The impedance diagrams were plotted every hour using a sinusoidal perturbation with an amplitude of 60 mA. The acquisition conditions for the diagrams were identical to those indicated above for the Ni–Cd battery. Measurement of the battery voltage before and after plotting of the impedance diagram was used to check whether its operation was quasi-stationary (Fig. 9).

The resulting diagrams, corrected in their high-frequency inductive part, are made up of two capacitive arcs in the 650 Hz–50 mHz frequency range. The size of the arc changes with the battery discharge level (Fig. 10). As was the case for the Ni–Cd batteries, the value of $R_c + R_i$, obtained by extrapolating the high-frequency arc, was practically constant during the discharge of the sealed lead/acid battery and increased at the end of the discharge (Fig. 11).

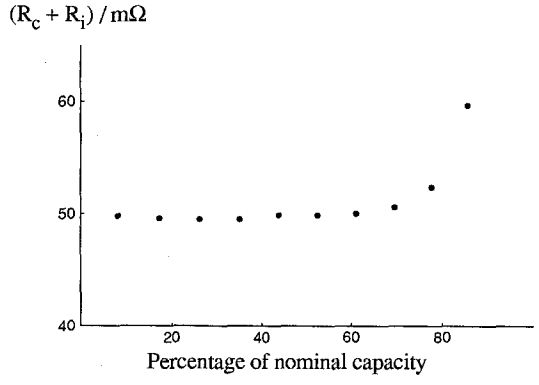

Fig. 11. $R_c + R_i$ evolution vs. percentage of nominal capacity for a Hawker sealed lead/acid Cyclon type BC 25 Ah 2 V cell discharged through a 1 Ω constant load.

5. Conclusions

We have proposed, developed and tested a new experimental method for impedance measurements of electrochemical batteries during discharge. This method uses a classical impedance-measurement set to control, under sinusoidal current perturbation, a battery connected in parallel to the load into which it discharges.

Impedance measurements were carried out on Mazda sealed Ni–Cd type NCR6 0.65 Ah batteries using the classical modulated-current method and the proposed method. The results show that the impedance diagrams, obtained during battery discharge through a constant load R, are identical to those obtained during discharges at a constant current with value U_{mean}/R where U_{mean} is the mean voltage of the battery during its natural discharge. These comparative measurements validate the proposed impedance-measurement method, which can be used to test all types of batteries or fuel cells.

Impedance measurements using the new method were carried out on a Hawker sealed lead/acid Cyclon type BC 25 Ah 2 V cell during discharge through a 1 Ω constant

load. The battery discharge current was then greater than the maximum value (2 A) that could be supplied by the regulation system. The constant-current measurement method could therefore not be used. The amplitude of the sinusoidal signal (60 mA) used during this study represented 2% of the mean value of the discharge current. The obtained results show that it is possible, using the method proposed in this article, to study with classical impedance-measurement set, the impedance of high-power and low-impedance batteries during their discharge through a constant load or more generally through an impedance $Z_R(\nu)$ which verifies the condition $Z_G(\nu) < Z_R(\nu)$ in the whole frequency domain.

Impedance diagrams of lead/acid and Ni–Cd batteries are made of high frequency inductive and resistive parts and two capacitive arcs. It is generally assumed [3] that the inductive part is due to the electrode geometry and connections inside the cell and that high frequency resistance is due to the connections, the separator and the electrolyte resistivity. The first capacitive loop is related to the electrode porosity and the second depends on electrode reaction kinetics controlled by mass transport [3].

Note that our article is focused on the method and operating mode for EIS measurements carried out with electrochemical batteries. Explanation of the impedance diagrams is beyond the scope of this work.

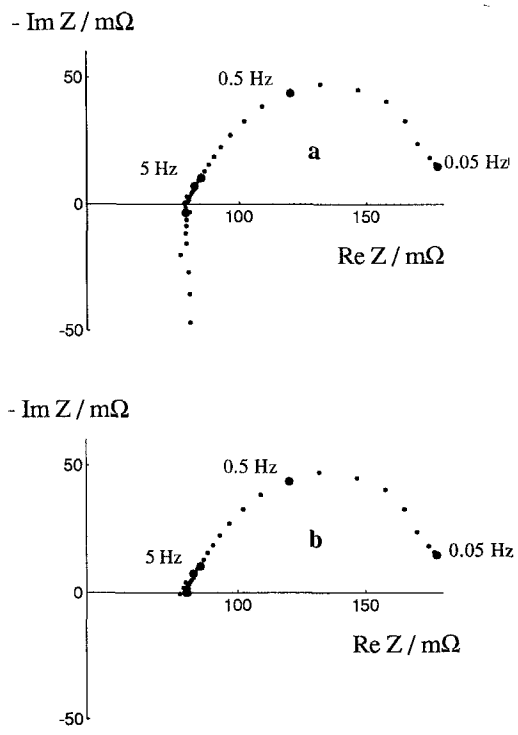

Fig. 12. Nyquist impedance diagram for a Mazda Ni–Cd type NCR6 0.65 Ah battery: (a) plotted at point A in Fig. 4 (discharge through a 30 Ω constant load), and (b) following correction of the high-frequency inductive part with $\Delta I = 2$ mA, $\nu \in$ [6500 Hz, 50 mHz]. The frequency is indicated on the diagrams.

Appendix A

The impedance diagrams for batteries during discharge often show inductive behaviour for the high frequencies, as is shown in the impedance diagram for a Mazda Ni–Cd type NCR6 0.65 Ah battery measured in the 6500 Hz–50 mHz frequency range following discharge of 46% of its nominal capacity through a 30 Ω constant load (Fig. 12(a) and point A on the diagram in Fig. 4). In this experiment, the connections between the measurement set and the battery were those presented in Fig. 1(b) and the amplitude of the sinusoidal signal was 2 mA.

The inductive behaviour at high frequencies depends on the battery studied as well as on the measurement set and the connections with the battery [1,5,12]. Certain authors have suggested running a blank test in which the battery is replaced by a resistor with a resistance equal to the low-frequency limit of its impedance and using the resulting diagrams to correct the impedance diagram for the battery [5].

We consider that the resulting diagrams are due to the combination of the battery impedance in series with an inductance or to a circuit formed by the parallel combination of an inductance and a resistance. For example, for the Mazda Ni–Cd type NCR6 0.65 Ah battery, the imaginary high-frequency part of the impedance diagrams varies in a linear manner with the frequency (Fig. 13) and the measured impedance is that of the battery in series with an inductance. The value measured at different discharge levels of the battery remains constant throughout a given experiment. The mean value of the inductance obtained from eight impedance diagrams during the discharge of the Ni–Cd battery through a 30 Ω constant load with a mean current of 41.3 mA and an amplitude modulation of 2 mA was 7.6 μH. This value was used to correct the impedance diagrams (Fig. 12(b)).

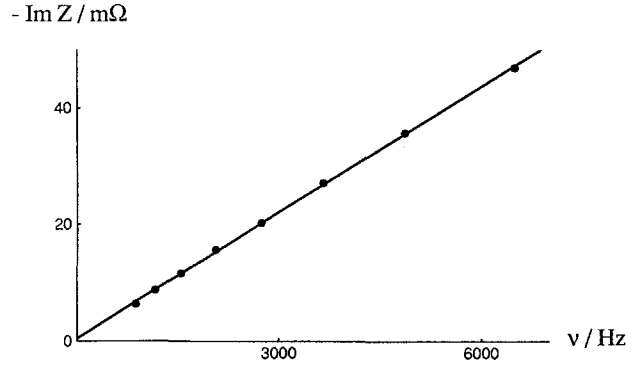

Fig. 13. High-frequency impedance imaginary part vs. frequency for the impedance diagram in Fig. 12(a): (●) experimental results are fitted to a (————) self-inductance impedance.

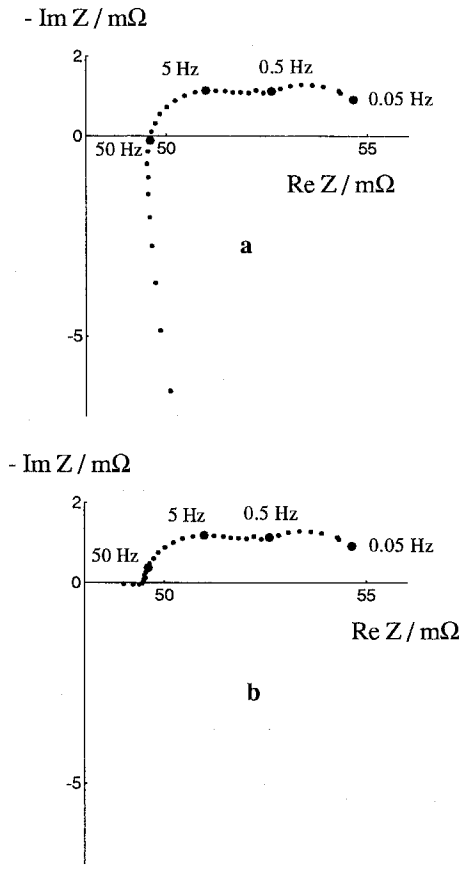

Fig. 14. Nyquist impedance diagram for a Hawker sealed lead/acid Cyclon type BC 25 Ah 2 V cell: (a) plotted at point D in Fig. 9 (discharge through a 1 Ω constant load), and (b) following correction of the high-frequency R_{HF}/L_{HF} part with $\Delta I = 60$ mA, $\nu \in$ [650 Hz, 50 mHz], the frequency is indicated on the diagrams.

For the Hawker sealed lead/acid Cyclon type BC cell 25 Ah 2 V cell, the imaginary high-frequency part of the impedance diagrams does not vary in a linear manner with the frequency, as is shown in the example in Fig. 14(a). The impedance is that of the battery in series with a circuit made up of an inductance and a resistance in parallel. The value of these components was measured by parametric identification of the imaginary high-frequency part of this circuit and that of the measured impedance. The value obtained for the inductance during discharge is approximately constant and the value of the resistance R_{HF} increases with the battery discharge level. The mean value of the inductance obtained on the basis of eight impedance diagrams during the discharge of the sealed lead/acid battery through a 1 Ω constant load was 1.6 μH. The determined L_{HF} and R_{HF} values were used to correct the impedance diagrams (Fig. 14(b)).

The determined values of L_{HF} (Ni–Cd battery) or of L_{HF} and R_{HF} (sealed lead/acid battery) may vary from 10 to 20% during successive experiments between which the battery connections are modified. This confirms that the inductive behaviour observed at high frequencies depends on the measurement set and on the system connections.

References

[1] C. Gabrielli, Tech. Rep. CSB/ A01, Schlumberger Technologies Instrument Division, 1990, Farnborough, Hampshire, UK.
[2] M. Hughes, S.A.G.R. Karunathilaka and N.A. Hampson, J. Appl. Electrochem., 13 (1983) 217; 14 (1984) 47.
[3] F. Huet, 10e Forum sur les Impédances Électrochimiques, Paris, France, 1996, p. 1.
[4] S. Sathyanarayana, S. Venugopalan and M.L. Gopikanth, J. Appl. Electrochem., 9 (1979) 125.
[5] S.A.G.R. Karunathilaka, R. Barton, M. Hughes and N.A. Hampson, J. Appl. Electrochem., 15 (1985) 251.
[6] J. Jindra, M. Musilová and J. Mrha, J. Power Sources, 37 (1992) 403.
[7] D. Lahav and J. Appelbaum, J. Power Sources, 38 (1992) 295.
[8] Ph. Blanchard, J. Appl. Electrochem., 22 (1992) 1121.
[9] R.S. Robinson, J. Power Sources, 42 (1993) 381.
[10] J.-P. Diard, B. Le Gorrrec and C. Montella, 5e Forum sur les Impédances Électrochimiques, Montrouge, France, 1991, p. 145.
[11] S. Wolfram, Mathematica, Addison Wesley, Reading, MA, 1988.
[12] B. Savova-Stoynov and Z. Stoynov, J. Appl. Electrochem., 17 (1987) 1150.